Pacific Graphics 2023
R. Chaine, Z. Deng, and M. H. Kim
(Guest Editors)

COMPUTER GRAPHICS *forum*
Volume 42 (2023), Number 7

Additional Material: Enhancing Low-Light Images: A Variation-based Retinex with Modified Bilateral Total Variation and Tensor Sparse Coding

Weipeng Yang[1], Hongxia Gao[†,1,2], Wenbin Zou[1], Shasha Huang[1], Hongsheng Chen[1], Jianliang Ma[1,3]

[11]School of Automation Science and Engineering, South China University of Technology, Guangzhou, China
[2]Research Center for Brain-Computer Interface, Pazhou Laboratory, Guangzhou, China
[3]KUKA Robotics Guangdong Co., Ltd., Foshan, China

Abstract

In this additional material, we have expanded upon our experimentation in greater detail. Firstly, to provide a more precise assessment of the noise suppression capabilities of our proposed BTRetinex model, we conducted experiments using LOL-v1 and LOL-v2 datasets. Secondly, as a commonly used no-reference image evaluation metric in low-light image enhancement tasks, we have included NIQE (Natural Image Quality Evaluator) results for various methods on the MixPG660 dataset. Thirdly, to analyze the impact of parameters on model performance, we have conducted a parameter study for the BTRetinex model. Lastly, we performed experiments on the VV dataset, which features high-resolution images, enabling more accessible visual comparisons. Code, dataset and experimental results are available at https://github.com/YangWeipengscut/BTRetinex.

1. Experiments on the LOL-v1 and LOL-v2 Datasets

We conducted experiments using the LOL-v1 [WWYL18] and LOL-v2 [YWH*21] datasets, each consisting of 15 and 100 paired test images, respectively. As our method is unsupervised, we only compared it with other unsupervised methods, namely WVM, Jiep, STAR, PnPRetinex, ZeroDCE and SCI, using PSNR and SSIM [WBSS04] metrics for evaluating noise suppression performance. Furthermore, since the majority of images in the LOL dataset have extremely low brightness, to achieve effective brightness enhancement, we set the gamma correction parameter for all Retinex-based methods to 2.6, instead of the commonly used 2.2.

The model parameters remain consistent with those stated in our paper, with parameters λ_1, λ_2 and λ_3 set to 0.002, 0.005 and 10^{-6}, respectively. We denote this parameter configuration as "Base". The quantitative results on these two datasets and the visual comparisons are presented in Table 1, Figure 1, Figure 2 and Figure 3, respectively. In the subsequent text, the numbers highlighted in bold red, bold green and bold blue correspond to the best, second-best and third-best results, respectively.

As observed from Table 1, under the Base parameter configuration, the proposed BTRetinex model achieves optimal results in both PSNR and SSIM metrics, indicating its superior noise suppression performance. Concurrently, from Figures 1, 2 and 3, it can be discerned that the LR3M method exhibits unstable brightness enhancement and excessive smoothing of the enhanced image details. The enhancement results of WVM, JieP and STAR methods display inadequate or inaccurate brightness enhancement (as evidenced by the black artifacts surrounding the digits of the clock in Figure 2). Moreover, the enhancement results from the PnPRetinex method exhibit a considerable number of erroneous red pixels (visible in both Figure 1 and Figure 3).

2. Experiments on the *MixPG660* Dataset

In addition to utilizing the ILNIQE, NIQMC and VIF metrics, we integrated the NIQE [MSB12] metric. The NIQE metric is a commonly used evaluation metric in the field of low-light image enhancement, where a smaller value indicates higher image quality. The quantitative results on this dataset and visual comparisons are presented in Table 2 and Figure 4, respectively.

As evident from Table 2, learning-based methods such as LLFlow, URetinex and SCI consistently rank first or second in terms of ILNIQE, NIQMC and NIQE metrics, showcasing favorable results in these evaluation metrics. However, their performance in the VIF metric is comparatively modest, implying a reduced fidelity of visual information. This tendency is reflected in their visual outcomes, as depicted in Figure 4. Notably, the SCI method tends to exhibit pronounced over-enhancement, while the URetinex and LLFlow methods often result in severe color distortion, prominent artifacts, or over-enhancement.

Table 1: *Quantitative comparison on the LOL-v1 and LOL-v2 datasets in terms of PSNR and SSIM.*

Dataset	LOL-v1		LOL-v2	
Metric	PSNR↑	SSIM↑	PSNR↑	SSIM↑
WVM	13.148	0.551	15.878	0.568
JiePG	13.435	0.567	16.250	0.584
STAR	14.242	**0.587**	17.150	**0.586**
LR3M	10.223	0.399	13.411	0.508
PnPRetinex	14.754	**0.597**	**17.463**	0.580
ZeroDCE	**14.861**	0.585	**18.059**	**0.603**
SCI	**14.784**	0.523	17.304	0.555
BTRetinex(Base)	**15.291**	**0.611**	**18.171**	**0.621**

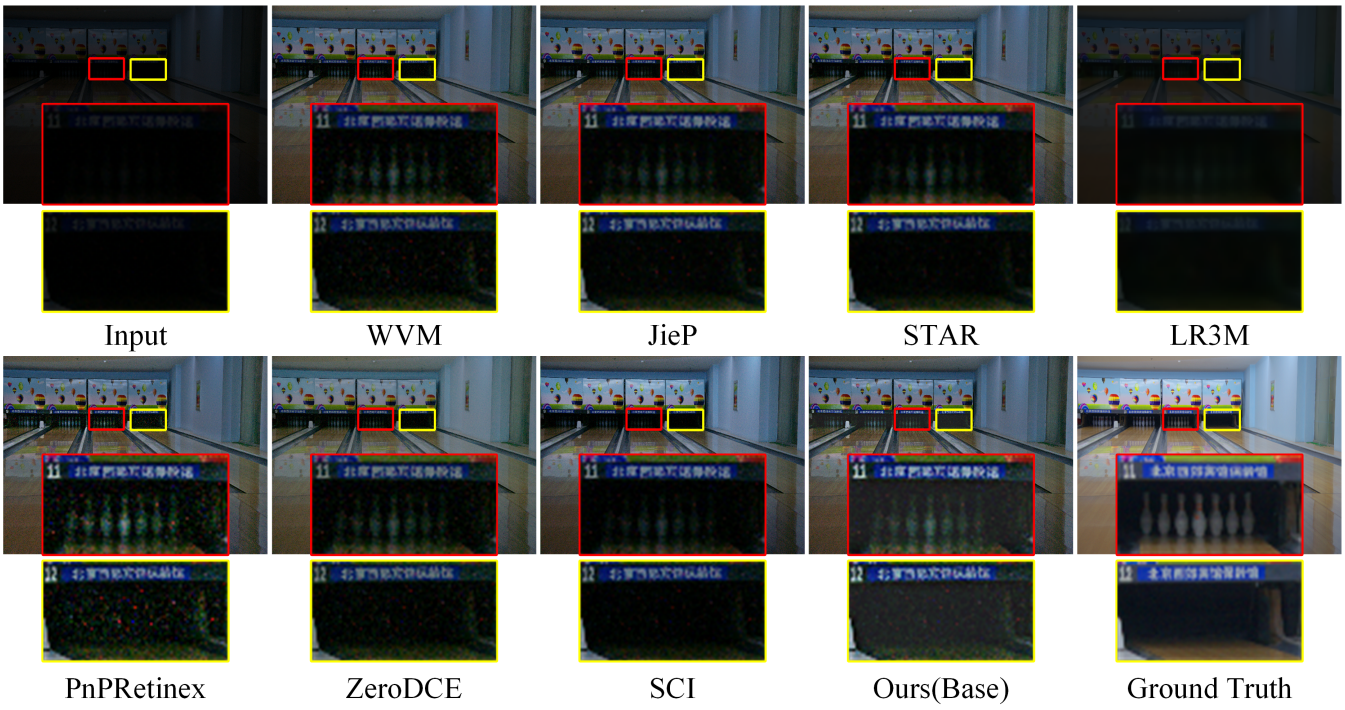

Figure 1: *Visual comparison of various low-light image enhancement methods on an image from the LOL-v1 dataset, including WVM [FZH*16], JieP [CXG*17], STAR [XHR*20], LR3M [RYCL20], PnPRetinex [LL22], ZeroDCE [GLG*20] and SCI [MML*22].*

As established in Section 3 through our parameter study, the rationale behind adopting the Base parameter configuration for our proposed BTRetinex model lies in achieving a harmonious balance between effective noise suppression and compelling visual results. If considering image evaluation metrics alone, the parameter settings of Case-4 yield improved comprehensive scores for our proposed model. Specifically, within this context, our model achieves the optimal value in the NIQE metric and ranks second in the ILNIQE metric. Additionally, under the parameter configurations of Case-7 and Case-8, there is also an observed improvement in the NIQMC and VIF metrics.

3. Parameter Study

In this section, we assess the impact of various values of the regularization parameters, namely λ_1, λ_2 and λ_3, on the performance of the proposed BTRetinex model. Table 3 presents 8 distinct sets of values for the model's regularization parameters. Tables 4 and 5 showcase the quantitative results of the proposed model on the LOL-v1, LOL-v2 and *MixPG660* datasets.

In the Base, Case-1, Case-2, Case-3 and Case-4 configurations, we maintained the values of λ_1 and λ_2 while varying the parameter λ_3. Analyzing the results from the LOL-v2 dataset, which encompasses a larger test image pool (100 paired images), it becomes apparent that

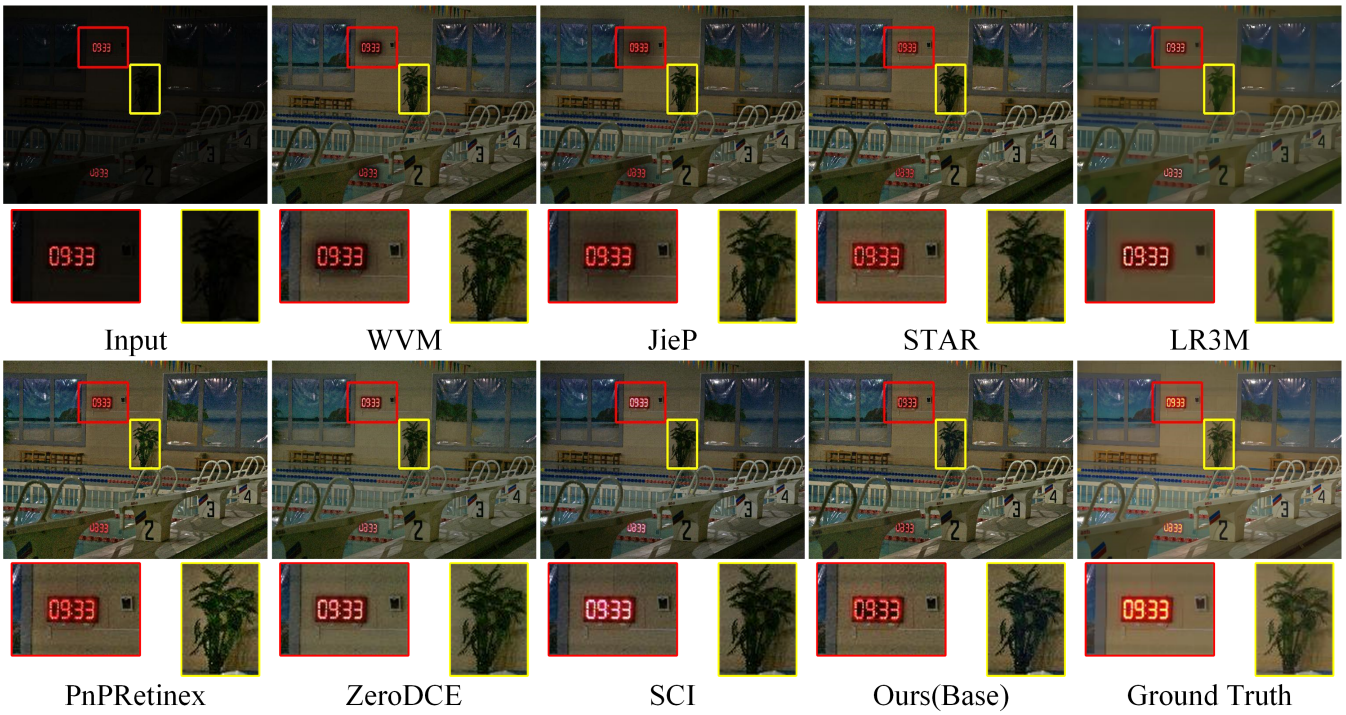

Figure 2: *Visual comparison of various low-light image enhancement methods on an image from the LOL-v1 dataset, including WVM [FZH*16], JieP [CXG*17], STAR [XHR*20], LR3M [RYCL20], PnPRetinex [LL22], ZeroDCE [GLG*20] and SCI [MML*22].*

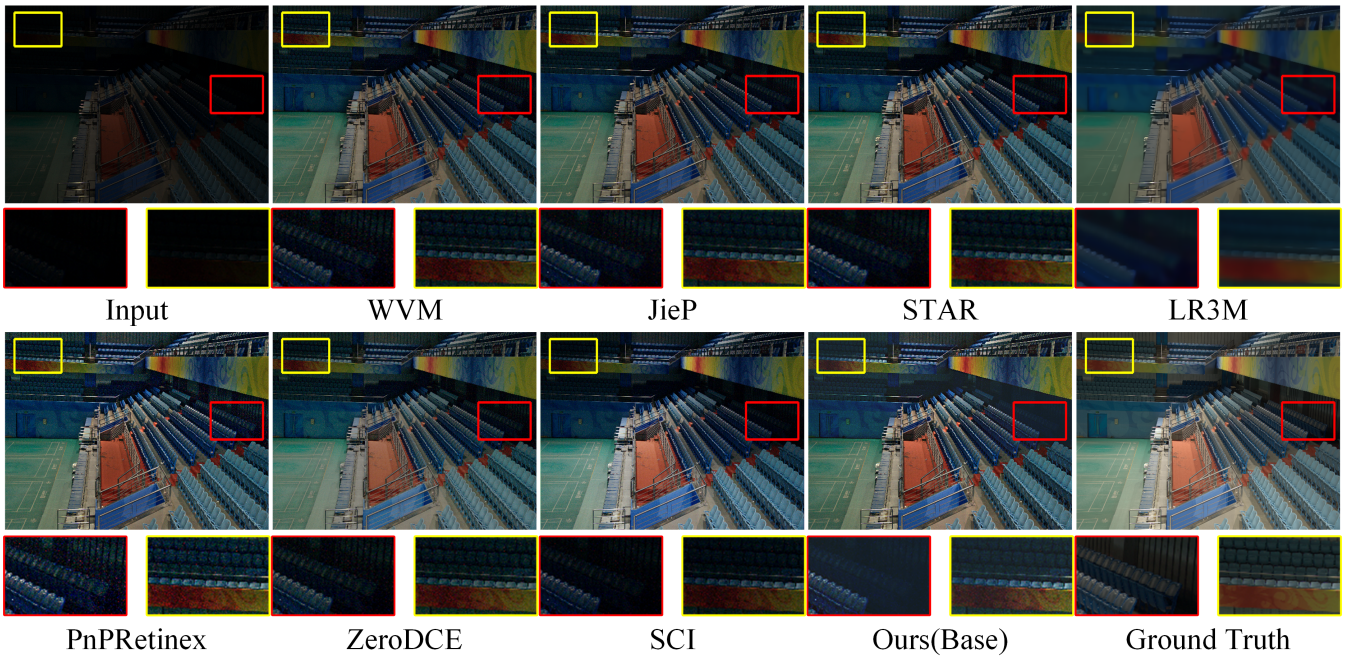

Figure 3: *Visual comparison of various low-light image enhancement methods on an image from the LOL-v2 dataset, including WVM [FZH*16], JieP [CXG*17], STAR [XHR*20], LR3M [RYCL20], PnPRetinex [LL22], ZeroDCE [GLG*20] and SCI [MML*22].*

Table 2: *Quantitative comparison on the MixPG660 dataset*

Metric	ILNIQE↓	NIQMC↑	VIF↑	NIQE↓
Input	27.445	4.508	1.000	3.449
WVM	26.153	4.683	1.315	**3.315**
JieP	25.517	4.732	**1.319**	**3.386**
STAR	25.836	4.804	1.212	3.425
LR3M	27.909	4.842	0.782	3.628
PnPRetinex	25.998	**4.999**	**1.520**	3.703
ZeroDCE	25.545	4.930	1.260	3.727
SCI	26.875	**5.278**	1.229	3.956
URetinex	**24.008**	5.166	1.074	3.597
LLFlow	**23.062**	**5.293**	1.171	**3.227**
BTRetinex(Base)	**24.819**	4.939	**1.328**	3.612

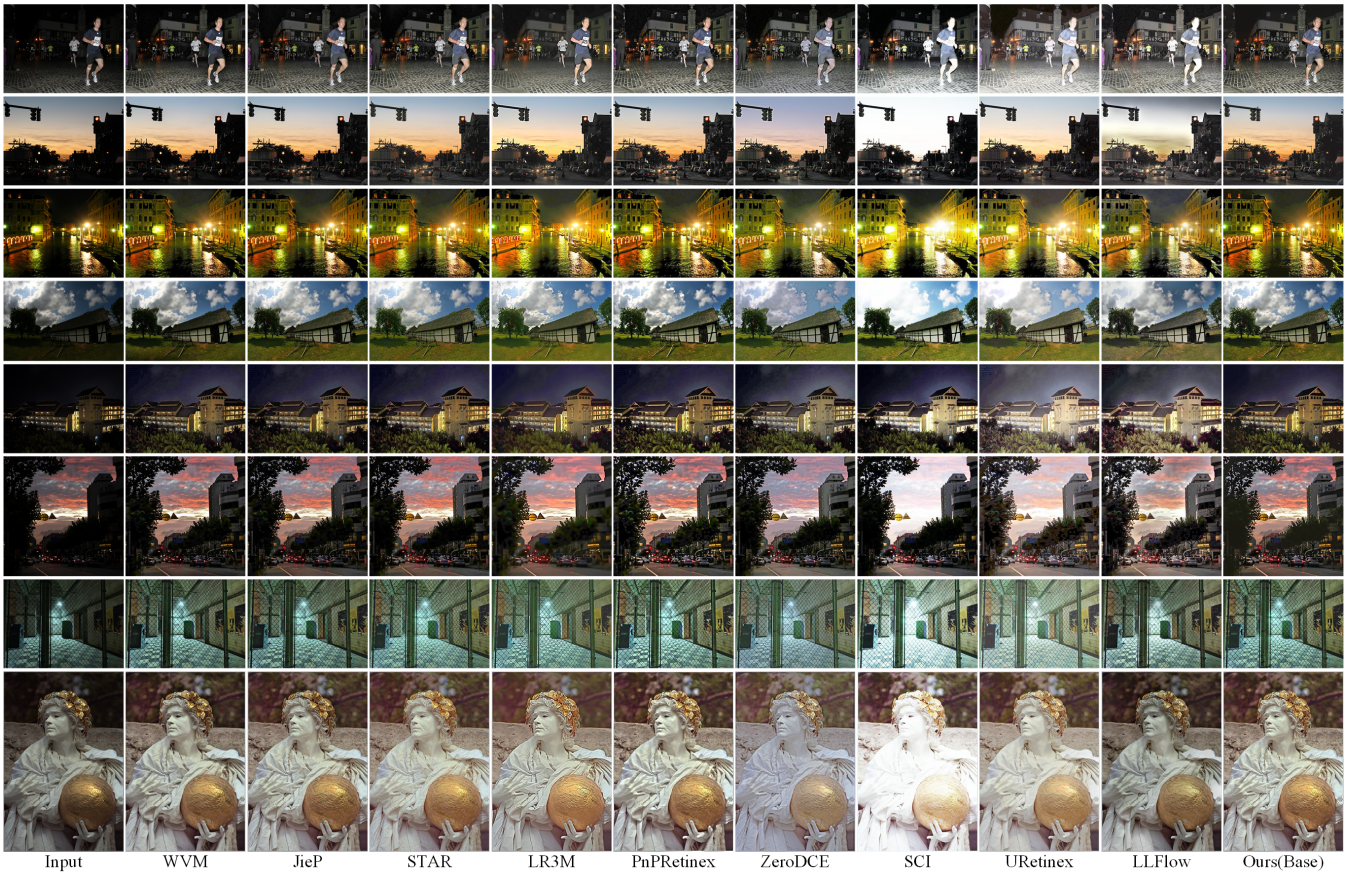

Figure 4: *Visual comparison of various low-light image enhancement methods on images from the MixPG660 dataset, including WVM [FZH*16], JieP [CXG*17], STAR [XHR*20], LR3M [RYCL20], PnPRetinex [LL22], ZeroDCE [GLG*20], SCI [MML*22], URetinex [WWZ*22] and LLFlow [WWY*22].*

Table 3: *Different values of regularization parameters for the proposed BTRetinex model*

Parameter	λ_1	λ_2	λ_3
BTRetinex(Base)	0.002	0.005	1e-06
Case-1	0.002	0.005	1e-08
Case-2	0.002	0.005	1e-04
Case-3	0.002	0.005	0.001
Case-4	0.002	0.005	0.01
Case-5	0.0002	0.005	1e-06
Case-6	0.02	0.005	1e-06
Case-7	0.002	0.0005	1e-06
Case-8	0.002	0.05	1e-06

Table 4: *Parameter study on the LOL-v1 and LOL-v2 datasets in terms of PSNR and SSIM.*

Dataset	LOL-v1		LOL-v2	
Metric	**PSNR↑**	**SSIM↑**	**PSNR↑**	**SSIM↑**
BTRetinex(Base)	**15.291**	**0.611**	18.171	0.621
Case-1	13.645	0.449	18.172	0.621
Case-2	13.668	0.473	18.376	**0.656**
Case-3	**15.295**	**0.639**	**18.585**	**0.669**
Case-4	15.203	**0.632**	**18.578**	**0.665**
Case-5	13.378	0.457	17.826	0.620
Case-6	**15.665**	0.592	**18.415**	0.601
Case-7	15.148	0.595	17.778	0.582
Case-8	13.610	0.465	18.480	0.644

as λ_3 increases, the model's PSNR and SSIM values exhibit an upward trend. This trend indicates an enhanced noise suppression capability of the model with the increment of λ_3. Nevertheless, excessively large λ_3 values lead to a loss of image details and adversely affect the VIF metric on the PG660 dataset, indicating a decline in the visual quality of the enhanced images. Consequently, we adopt the λ_3 value of 1.0e-6 from the Base parameter configuration.

In the Base, Case-5 and Case-6 configurations, we maintained the values of λ_2 and λ_3 while varying the parameter λ_1. As evidenced by the NIQMC and VIF values in Table 5, increasing λ_1 primarily serves to enhance the contrast and visual information fidelity of the enhanced images. However, it is worth noting that excessive λ_1 values lead to a loss of image details, manifesting in the lower SSIM value in Case-6 in Table 4 compared to the SSIM value in the Base configuration. Therefore, we adopt the λ_1 value of 0.002 from the Base parameter configuration.

In the Base, Case-7 and Case-8 configurations, we maintained the values of λ_1 and λ_3 while varying the parameter λ_2. As demonstrated by the NIQMC and VIF values in Table 5, reducing λ_2 primarily enhances the contrast and visual information fidelity of the enhanced images. However, it is important to note that excessively small λ_2 values can lead to a reduction in the noise suppression performance of the model, as evident in Case-7 in Table 4, where both PSNR and SSIM values are lower than those in the Base configuration. Therefore, we set the value of λ_2 to 0.002 from the Base parameter configuration.

Table 5: *Parameter study on the MixPG660 dataset*

Metric	ILNIQE↓	NIQMC↑	VIF↑	NIQE↓
BTRetinex(Base)	24.819	4.939	1.328	3.612
Case-1	24.868	4.939	**1.334**	3.610
Case-2	**23.983**	4.933	1.215	**3.459**
Case-3	**23.735**	4.924	1.161	**3.262**
Case-4	**23.774**	**4.952**	1.131	**3.207**
Case-5	25.182	4.732	1.154	3.795
Case-6	25.132	**5.186**	**1.392**	3.542
Case-7	25.184	**5.018**	**1.417**	3.631
Case-8	25.049	4.691	1.070	3.503

4. Experiments on the VV Dataset

To facilitate more effective visual comparisons, experiments were also conducted on the VV dataset [Von17]. The VV dataset comprises 24 of the most challenging images captured during Vassilios Vonikakis' everyday experiences. Within this dataset, each image showcases a section that is correctly exposed, alongside another section that exhibits significant under/over-exposure. The images in this dataset possess a resolution of around 2300×1700. The visual comparisons are presented in Figure 5 and 6. As illustrated in these figures, it is apparent that our model not only efficiently suppresses noise but also achieves noteworthy improvements in visual quality.

The LR3M method consumes a substantial amount of memory (approximately 51GB) when processing images from the VV dataset. Furthermore, based on the experimental results obtained from the LOL-v1 and LOL-v2 datasets, it becomes evident that the performance of this method is subpar, as it tends to smooth out a significant portion of image detail. Therefore, we have chosen not to include the results of the LR3M method in this section.

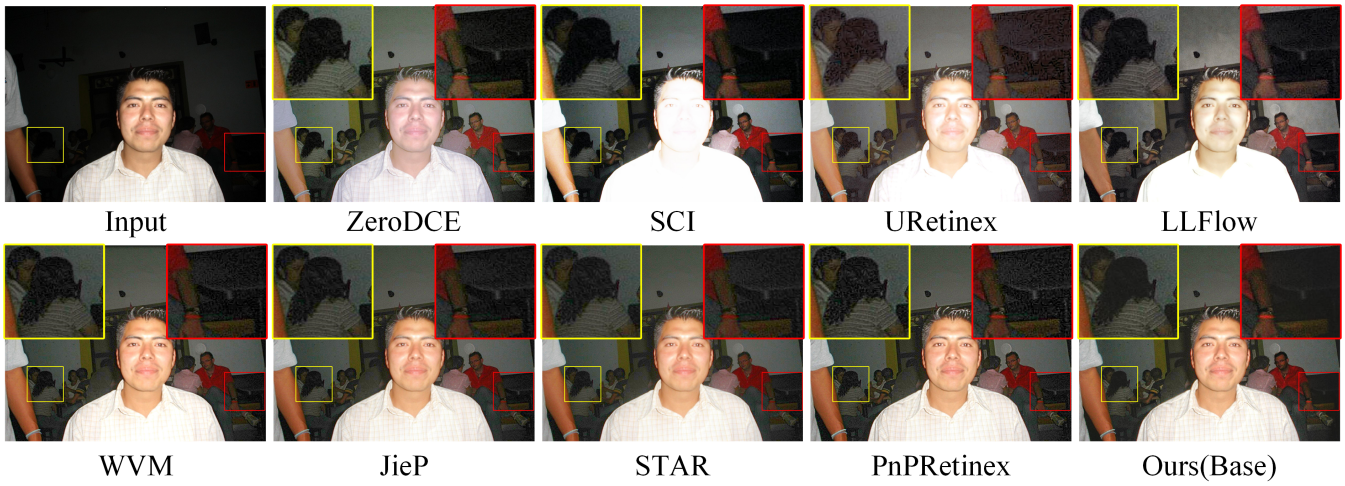

Figure 5: *Visual comparison of various low-light image enhancement methods on an image from the VV dataset, including ZeroDCE [GLG*20], SCI [MML*22], URetinex [WWZ*22], LLFlow [WWY*22], WVM [FZH*16], JieP [CXG*17], STAR [XHR*20] and PnPRetinex [LL22].*

Figure 6: *Visual comparison of various low-light image enhancement methods on an image from the VV dataset, including ZeroDCE [GLG*20], SCI [MML*22], URetinex [WWZ*22], LLFlow [WWY*22], WVM [FZH*16], JieP [CXG*17], STAR [XHR*20] and PnPRetinex [LL22].*

References

[CXG*17] CAI B., XU X., GUO K., JIA K., HU B., TAO D.: A joint intrinsic-extrinsic prior model for retinex. In Proceedings of the IEEE international conference on computer vision (2017), pp. 4000–4009. 2, 3, 4, 6

[FZH*16] FU X., ZENG D., HUANG Y., ZHANG X.-P., DING X.: A weighted variational model for simultaneous reflectance and illumination estimation. In Proceedings of the IEEE conference on computer vision and pattern recognition (2016), pp. 2782–2790. 2, 3, 4, 6

[GLG*20] GUO C., LI C., GUO J., LOY C. C., HOU J., KWONG S., CONG R.: Zero-reference deep curve estimation for low-light image enhancement. In Proceedings of the IEEE/CVF conference on computer vision and pattern recognition (2020), pp. 1780–1789. 2, 3, 4, 6

[LL22] LIN Y.-H., LU Y.-C.: Low-light enhancement using a plug-and-play retinex model with shrinkage mapping for illumination estimation. IEEE Transactions on Image Processing 31 (2022), 4897–4908. 2, 3, 4, 6

[MML*22] MA L., MA T., LIU R., FAN X., LUO Z.: Toward fast, flexible, and robust low-light image enhancement. In Proceedings of the IEEE/CVF Conference on Computer Vision and Pattern Recognition (2022), pp. 5637–5646. 2, 3, 4, 6

[MSB12] MITTAL A., SOUNDARARAJAN R., BOVIK A. C.: Making a "completely blind" image quality analyzer. IEEE Signal processing letters 20, 3 (2012), 209–212. 1

[RYCL20] REN X., YANG W., CHENG W.-H., LIU J.: Lr3m: Robust low-light enhancement via low-rank regularized retinex model. IEEE Transactions on Image Processing 29 (2020), 5862–5876. 2, 3, 4

[Von17] VONIKAKIS. V.: Busting Image Enhancement and Tone-Mapping Algorithms: A Collection of the Most Challenging Cases, 2017. (2017). URL: https://sites.google.com/site/vonikakis/datasets. 6

[WBSS04] WANG Z., BOVIK A. C., SHEIKH H. R., SIMONCELLI E. P.: Image quality assessment: from error visibility to structural similarity. IEEE transactions on image processing 13, 4 (2004), 600–612. 1

[WWY*22] WANG Y., WAN R., YANG W., LI H., CHAU L.-P., KOT A.: Low-light image enhancement with normalizing flow. In Proceedings of the AAAI Conference on Artificial Intelligence (2022), vol. 36, pp. 2604–2612. 4, 6

[WWYL18] WEI C., WANG W., YANG W., LIU J.: Deep retinex decomposition for low-light enhancement. arXiv preprint arXiv:1808.04560 (2018). 1

[WWZ*22] WU W., WENG J., ZHANG P., WANG X., YANG W., JIANG J.: Uretinex-net: Retinex-based deep unfolding network for low-light image enhancement. In Proceedings of the IEEE/CVF Conference on Computer Vision and Pattern Recognition (2022), pp. 5901–5910. 4, 6

[XHR*20] XU J., HOU Y., REN D., LIU L., ZHU F., YU M., WANG H., SHAO L.: Star: A structure and texture aware retinex model. IEEE Transactions on Image Processing 29 (2020), 5022–5037. 2, 3, 4, 6

[YWH*21] YANG W., WANG W., HUANG H., WANG S., LIU J.: Sparse gradient regularized deep retinex network for robust low-light image enhancement. IEEE Transactions on Image Processing 30 (2021), 2072–2086. 1